ACS OMEGA

http://pubs.acs.org/journal/acsodf

Article

Ability to Inhibit H^+ Transmission of Gemini Surfactants with Different Chain Lengths under Different Ca^{2+} Circumstances

Feng Zhao, Shibin Wang,* Jianchun Guo,* Yuheng Yang, Yuan Wang, Zhi Wang, and Peng Shi

Cite This: *ACS Omega* 2022, 7, 20768−20778

Read Online

ACCESS | Metrics & More | Article Recommendations

ABSTRACT: To study the ability to inhibit ion transmission of the Gemini surfactant under different Ca^{2+} circumstances, three kinds of Gemini surfactants with different alkyl chain lengths are synthesized (C*n*-4-C*n*, *n* = 12, 14, and 16), which are characterized using ^1H NMR, ^{13}C NMR, and Fourier transform infrared spectroscopy. To analyze the property of inhibition of the acid−rock reaction rate, surface tension and contact angle measurements and atomic force microscopy (AFM) results are obtained with different surfactants and under different Ca^{2+} concentrations. Inhibition rates with different alkyl chain lengths and an acid-etched surface morphology are also studied carefully. The result shows that all cationic Gemini surfactants significantly impact the control of the reaction rate, and the reaction rate decreased remarkably by 44.4% after adding 12-4-12. The ΔG and W_A indicate that 12-4-12 has the best adsorption ability on the rock with added Ca^{2+} compared with the other two Gemini surfactants. It is revealed through the AFM that Ca^{2+} can significantly change the adsorption morphology of the surfactant. The surfactant adsorption area decreased when Ca^{2+} is dispersed in the solution as well. These two phenomena can lead to the reduced ability to block H^+ of 14-4-14 and 16-4-16. However, the presence of Ca^{2+} affects the adsorption area of 12-4-12 slightly. Thus, the reaction rate, including that of 12-4-12, is almost unchanged. Because 12-4-12 is adsorbed tightly on the rock surface, H^+ can only react with the rock on the unabsorbed dot, resulting in rock surface nonuniformity after being etched, which is beneficial for maintaining the conductivity of the crack.

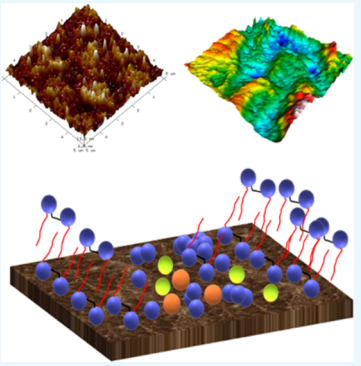

1. INTRODUCTION

As a new type of surfactant, Gemini surfactants are made up of two amphiphilic moieties linked by a spacer chain, which have been the focus of considerable research interest since the 1990s.[1] Gemini surfactants have lots of special physical and chemical properties, such as a lower critical micelle concentration (CMC), higher surface/interfacial activities, and numerous self-assembly morphologies, compared to the conventional surfactant.[2−5] This means that these surfactants have potential applications in many areas, including the petroleum industry, drug delivery, and corrosion.[6−9]

Generally, many researchers are interested in the effect of salt on the solution properties of the Gemini surfactant.[10−14] However, the research studies that pay attention to the influence of surfactants under different salt circumstances on the solid surfaces are relatively rare. Many papers have reported the surface morphology obtained using atomic force microscopy (AFM) depending on it to judge the ability of surfactants to change the property of the rock surface. These studies disclosed that the surface micelles of hexadecyltrimethylammonium chloride or bromide on mica become more curved as the salt concentration is increased. The reason is that the surfactant ion competes with the salt to adsorb onto the negatively charged sites on the rock surface.[15] Duval has shown that the aggregate on the rock of the cationic Gemini surfactant curvature also increases in the presence of salt, which is similar to that in conventional single-chain surfactants.[16]

Carbonate rock reservoirs, accounting for half of the world's oil and gas resources, are still one of the primary energy sources. Acid stimulation is commonly used to develop carbonate rock reservoirs.[17−19] Hydrochloric acid is considered the main stimulation fluid with its excellent dissolving power, low cost, and high solubility of products for acid fracturing.[20] One of the most critical points in carbonate acidizing treatments is inhibiting the acid−rock reaction rate. Commonly, three steps are recognized in the acid−rock reaction process: hydrogen ions are delivered to the rock surface through mass transfer; hydrogen ions are involved in the reaction at the surface of the rock; and the products leave the rock surface and move into the liquid.[21,22] Some high-viscosity fluids, such as gelled acids, emulsified acids, and surfactant-based acids, have been developed to inhibit the acid−rock reaction rate.[23−25] These acid systems for the

Received: March 3, 2022
Accepted: May 20, 2022
Published: June 7, 2022

https://doi.org/10.1021/acsomega.2c01253
ACS Omega 2022, 7, 20768−20778

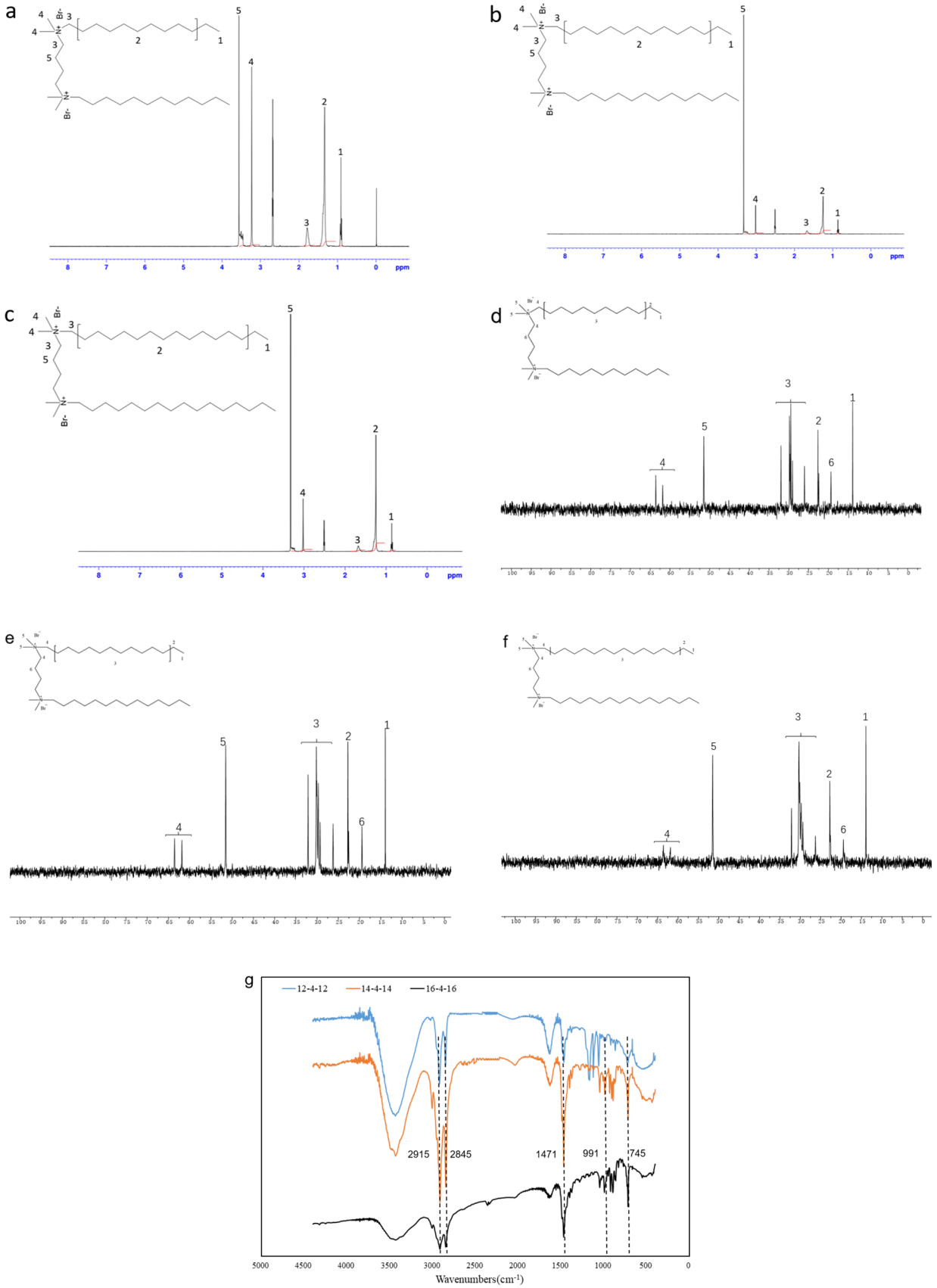

Figure 1. ^{1}H NMR spectra of the Gemini surfactants: (a) 12-4-12, (b) 14-4-14, and (c) 16-4-16, the ^{13}C NMR spectra of the Gemini surfactants: (d) 12-4-12, (e) 14-4-14, and (f) 16-4-16, and (g) IR spectra.

https://doi.org/10.1021/acsomega.2c01253
ACS Omega 2022, 7, 20768−20778

mechanism of inhibiting the reaction rate are mainly used in the first acid−rock reaction process by increasing the viscosity to reduce the transfer coefficient of H^+.[26−28]

However, there are a few researchers focusing on controlling reactions based on the second step of the acid−rock reaction process.[29,30] The surfactant has the ability to adsorb on the surface. Based on the theory of the acid−rock reaction process, the surfactant should play a special role in inhibiting the acid−rock reaction.

Metal ions can affect the performance of surfactants. Calcium carbonate is one of the main components of carbonate rock. Many calcium ions are produced from the acid rock reaction, which play a role in the inhibition of the acid−rock reaction rate. It is necessary to pay attention to the effect of Ca^{2+} on the interaction between the rock and surfactant.

In this study, a series of Gemini surfactants, 12-4-12, 14-4-14, and 16-4-16, are synthesized. Considering the formation of Ca^{2+} during the acid−rock reaction, surface tension and contact angle measurements and AFM with different Ca^{2+} concentrations are performed. The inhibition rate and surface morphology of the rock plate are obtained using etching tests. The results show that Gemini surfactants have good performance for potential application in acid fracturing.

2. RESULTS AND DISCUSSION

2.1. Characterization of the Synthesized Surfactants. The chemical structures of the synthesized surfactants 12-4-12, 14-4-14, and 16-4-16 are confirmed using ^{1}H NMR and ^{13}C NMR spectroscopy results. The ^{1}H NMR and ^{13}C NMR spectra are shown in Figure 1. The numbers on the hydrogen and carbon spectrum peaks correspond to the numbers of the functional groups in the structural diagram. For ^{1}H NMR, the presence of characteristic peaks at (δ) values of 0.841−0.875 ppm (12-4-12), 0.845−0.880 ppm (14-4-14), and 0.844−0.878 ppm (16-4-16) corresponds to the presence of terminal methyl groups constituting the long chain, that is, number 1. For ^{13}C NMR, the presence of characteristic peaks at (δ) values of 13.89 ppm (12-4-12), 13.91 ppm (14-4-14), and 13.9 (16-4-16) corresponds to number 1. For ^{1}H NMR, the presence of peaks at chemical shift (δ) values of 1.251−1.294 ppm (12-4-12), 1.251−1.298 ppm (14-4-14), and 1.247−1.297 ppm (16-4-16) is attributed to the existence of 9, 11, and 13 methylene groups adjacent to the terminal methyl groups, that is, number 2. Also, these methylene groups correspond to number 3 in the carbon spectrum, for which the values are 22.44−22.65 (12-4-12), 22.44−22.65 (14-4-14), and 22.76 (16-4-16). For ^{13}C NMR, the presence of characteristic peaks at (δ) values of 22.44−22.65 (12-4-12), 22.44−22.65 (14-4-14), and 22.76 (16-4-16) corresponds to the presence of methylene groups adjacent to the terminal methyl groups constituting the long chain, that is, number 2. For ^{1}H NMR, the presence of peaks at chemical shift (δ) values of 1.667−1.674 (12-4-12), 1.677 (14-4-14), and 1.671−1.681 (16-4-16) corresponds to the methylene group adjacent to the ammonium group in the long carbon chain and the space group, that is, number 3. Also, these methylene groups correspond to number 4 in the carbon spectrum, for which the values are 61.84−63.58 (12-4-12), 61.82−63.57 (14-4-14), and 61.84−63.59 (16-4-16). For ^{1}H NMR, the presence of peaks at chemical shift (δ) values of 3.031 (12-4-12), 3.016 (14-4-14), and 3.022 (16-4-16) correspond to the two methyl groups attached to the ammonium group, that is, number 4. Also, these methyl groups correspond to number 5 in the carbon spectrum, for which the values are 51.46 (12-4-12), 51.52 (14-4-14), and 51.5 (16-4-16). For ^{1}H NMR, the presence of peaks at chemical shift (δ) values of 3.245−3.287 (12-4-12), 3.228−3.312 (14-4-14), 3.232−3.286 (16-4-16) corresponds to the methylene group of the space group, that is, number 5. Also, these methylene groups correspond to number 6 in the carbon spectrum, for which the values are 19.38 (12-4-12), 19.43 (14-4-14), and 19.43 (16-4-16).

The infrared (IR) spectra of the three surfactants are shown in Figure 1g. 2915 and 2845 cm^{-1} are the stretching vibration peaks of C−H in $-CH_3$ and $-CH_2$-, respectively, and 1471 cm^{-1} is the bending vibration peak of C−H in $-CH_3$ and $-CH_2-$. 992 cm^{-1} is the stretching vibration peak of $N^+-(CH_3)_2$, and 722 cm^{-1} is the in-plane vibration absorption peak of the long methylene chain, indicating the existence of long-chain alkyl groups.

2.2. Surface Activities. The surface tension values of the surfactant solution as a function of the concentration are present in Figure 2. The CMC and γ_{cmc} values are summarized in Table 1. For the pure Gemini surfactant solution, the length of the carbon chain increases and the CMC of the surfactant gradually decreases, which is in good agreement with the available literature.[31]

In the Gemini surfactant/salt solutions, the addition of $CaBr_2$ can significantly reduce the CMC. The CMCs of the three kinds of Gemini surfactants reduced by more than 1 order of magnitude. The result is that the electrostatic repulsion between the intermolecular head groups is reduced by the counter ions, which leads to the promoted ability to form micelles.[32]

The change trend of the surface tension value of the Gemini surfactant is similar to that of their CMCs. Inorganic salts can reduce the surface tension of the solution slightly. In general, Ca^{2+} has less effect on surface tension.

2.3. Effect of Ca^{2+} on the Adsorption Morphology of the Gemini Surfactant. Figure 3 shows the structure of Gemini surfactant aggregates on the rock surface at different $CaBr_2$ concentrations and a constant Gemini surfactant concentration of 0.5 cmc. The left and middle pictures show the adsorption topography, and the right side shows the thickness of the adsorption layer corresponding to the red line. It is indicated from the topographic images that the Gemini surfactant on the rock surface changes significantly with the Ca^{2+} concentration increase.

For a pure Gemini surfactant solution, there are more and more aggregates of the surfactant on the rock surface as the length of the carbon chain increases (Figure 3a−c). The structure of 12-4-12 is dominated by a single layer of adsorption, which is interspersed with fine needle-shaped micelles. The structure of 14-4-14 is similar to that of 12-4-12, but the coverage area is less than that of 12-4-12. 16-4-16 is mainly composed of columnar micelles and mountain-shaped micelles. Compared with those in the previous work,[30] the density and area of the Gemini surfactant adsorption are greater than that of traditional surfactants.

With the increase in the concentration of Ca^{2+}, the aggregated structures of the three surfactants on the surface of the rock are evident, and the morphology of surfactants changed significantly. For 12-4-12 with 100 ppm Ca^{2+}, compared with the corresponding only Gemini surfactant, the volume of a single micelle is more extensive, and the aggregation is prominent (Figure 3a$_1$). Almost no monolayers

https://doi.org/10.1021/acsomega.2c01253
ACS Omega 2022, 7, 20768−20778

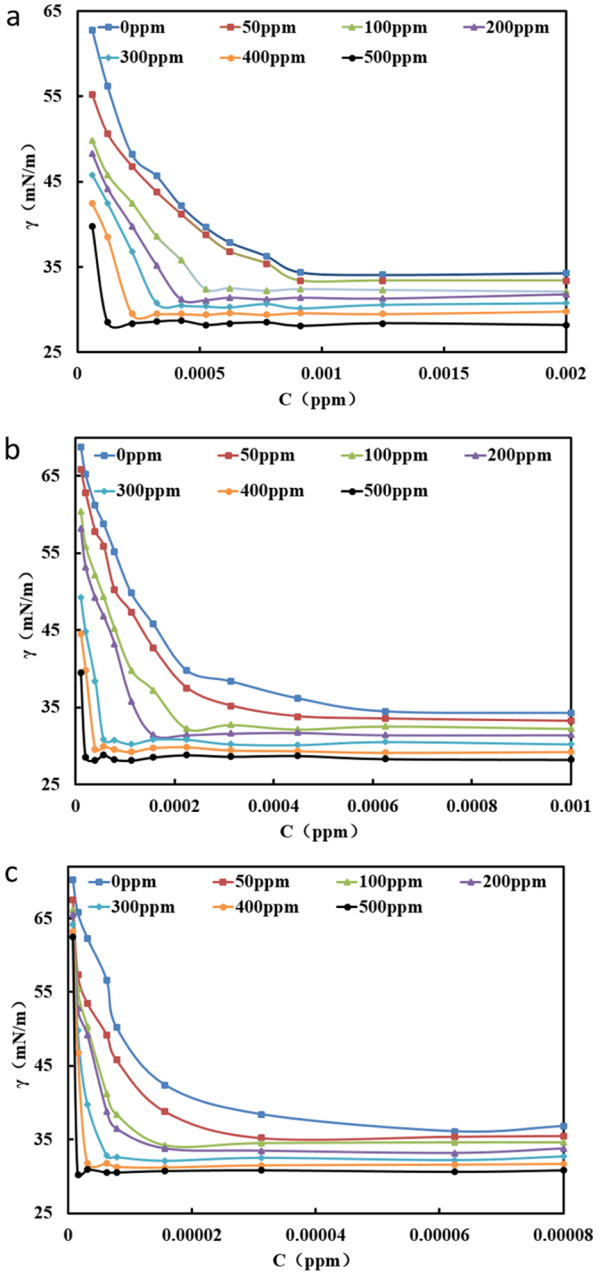

Figure 2. Surface tension vs Gemini surfactants with different $CaBr_2$ concentrations: (a) 12-4-12, (b) 14-4-14, and (c) 16-4-16.

can be observed clearly on the rock surface. The length of a single surfactant is about 2 nm.[33] The height of most micelles is the length of two−three surfactant molecules. When the concentration of Ca^{2+} is 300 ppm, the aggregate morphology changes from a single aggregate to a massive structure, and the area of the adsorption region is further reduced (Figure 3a_2). Under the same substrate, some areas have a large number of molecules and some areas have less molecules, showing extreme heterogeneity.

For 14-4-14, at the same concentration of Ca^{2+} as that of 12-4-12, the surfactant is more likely to form blocky aggregation in the solution (Figure 3b_1,b_2). In addition, 14-4-14 has a smaller adsorption area than 12-4-12 at the same Ca^{2+} concentration. For 16-4-16, it is indicated that the area of adsorption is significantly reduced, while the volume of a single cylinder micelle increases with the addition of Ca^{2+}(Figure 3c_1,c_2). Therefore, considering the relation between the morphology and adsorption area and the ability to block H^+, 12-4-12 shows the best inhibiting ability.

According to the above discussion, we propose the possible cartoon models of the adsorbed Gemini surfactant aggregates on the rock surface with different Ca^{2+} concentrations.

When $CaBr_2$ is added to the solution, Ca^{2+} and surfactant molecules both try to adsorb on the rock surface, resulting in a decrease in the area and density of the rock adsorbed by the surfactant, as shown in Figure 4.[15] Moreover, Ca^{2+} and Gemini surfactant head groups are positively charged, which leads to the inability to continue to adsorb surfactants in this area because of electrostatic repulsion power.

When the surfactant occupies the region, the neighboring regions favor adsorbing the surfactant molecular because of the hydrophobic effect. Furthermore, Br^- promotes the surfactant aggregation by shielding the repulsive electrostatic interactions between the surfactant's head groups. Meanwhile, with the increase in the concentration of inorganic salts, Ca^{2+} will occupy more surface of the rock and take the adsorption sites of the surfactant, resulting in more obvious surfactant aggregation and more complex adsorption forms. While the length of the carbon chain increases, the adsorption area and density gradually decrease at the same salt concentration. The increasing carbon chain length results in a stronger hydrophobic association between surfactants, enhancing the aggregation on rock surfaces.

2.4. Effect of Ca^{2+} on the Adsorption Ability of the Gemini Surfactant. To better understand the effect of Ca^{2+} on the adsorption ability of the Gemini surfactant on carbonate, the free energy of the surface (ΔG) and the work of adhesion (W_A) are evaluated, respectively. The free energy of the surface indicates the power of interaction between the spread liquid and the concrete surface.[34] Under a fixed temperature and pressure, the free energy values of solid surfaces are lower, which is more favorable for the solution of the surfactant spread on the rock surface. The work of

Table 1. CMC and γ_{cmc} Values of Gemini Surfactants with Various Concentrations of Ca^{2+} at 25 °C

	12-4-12		14-4-14		16-4-16	
$CaBr_2$ (ppm)	CMC (mol/L)	γ_{cmc} (mN/m)	CMC (mol/L)	γ_{cmc} (mN/m)	CMC (mol/L)	γ_{cmc} (mN/m)
0	9.12×10^{-4}	34.3	6.25×10^{-4}	34.3	6.25×10^{-5}	36.1
50	7.75×10^{-4}	33.4	4.48×10^{-4}	33.2	3.12×10^{-5}	35.4
100	5.25×10^{-4}	32.5	2.24×10^{-4}	32.2	1.56×10^{-5}	34.4
200	4.25×10^{-4}	31.8	1.12×10^{-4}	31.4	7.81×10^{-6}	33.4
300	3.13×10^{-4}	30.8	5.6×10^{-5}	30.2	6.25×10^{-6}	32.5
400	2.25×10^{-4}	29.8	3.91×10^{-5}	29.2	3.12×10^{-6}	31.9
500	1.25×10^{-4}	28.2	1.95×10^{-5}	28.2	1.56×10^{-6}	30.1

https://doi.org/10.1021/acsomega.2c01253
ACS Omega 2022, 7, 20768−20778

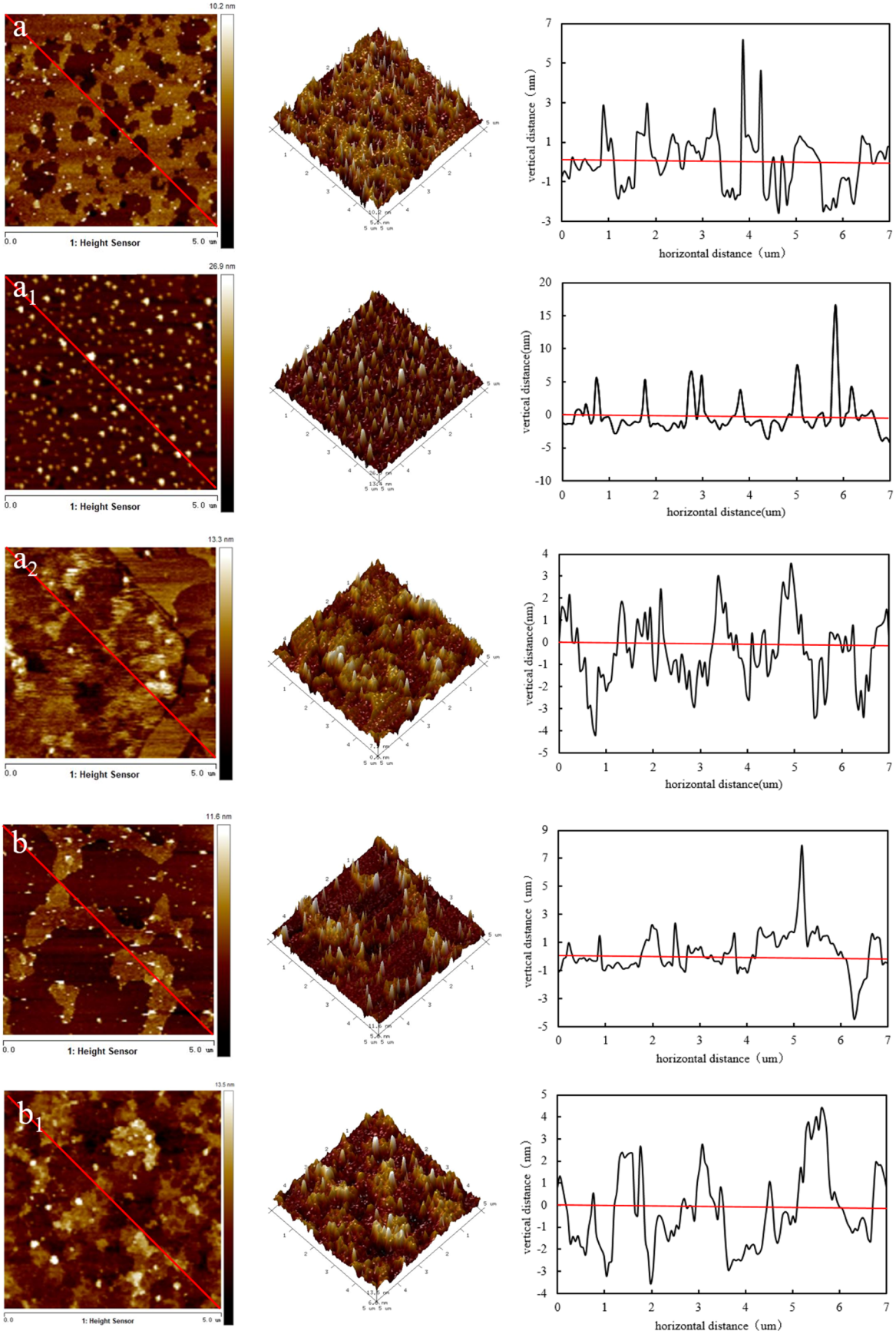

Figure 3. continued

https://doi.org/10.1021/acsomega.2c01253
ACS Omega 2022, 7, 20768−20778

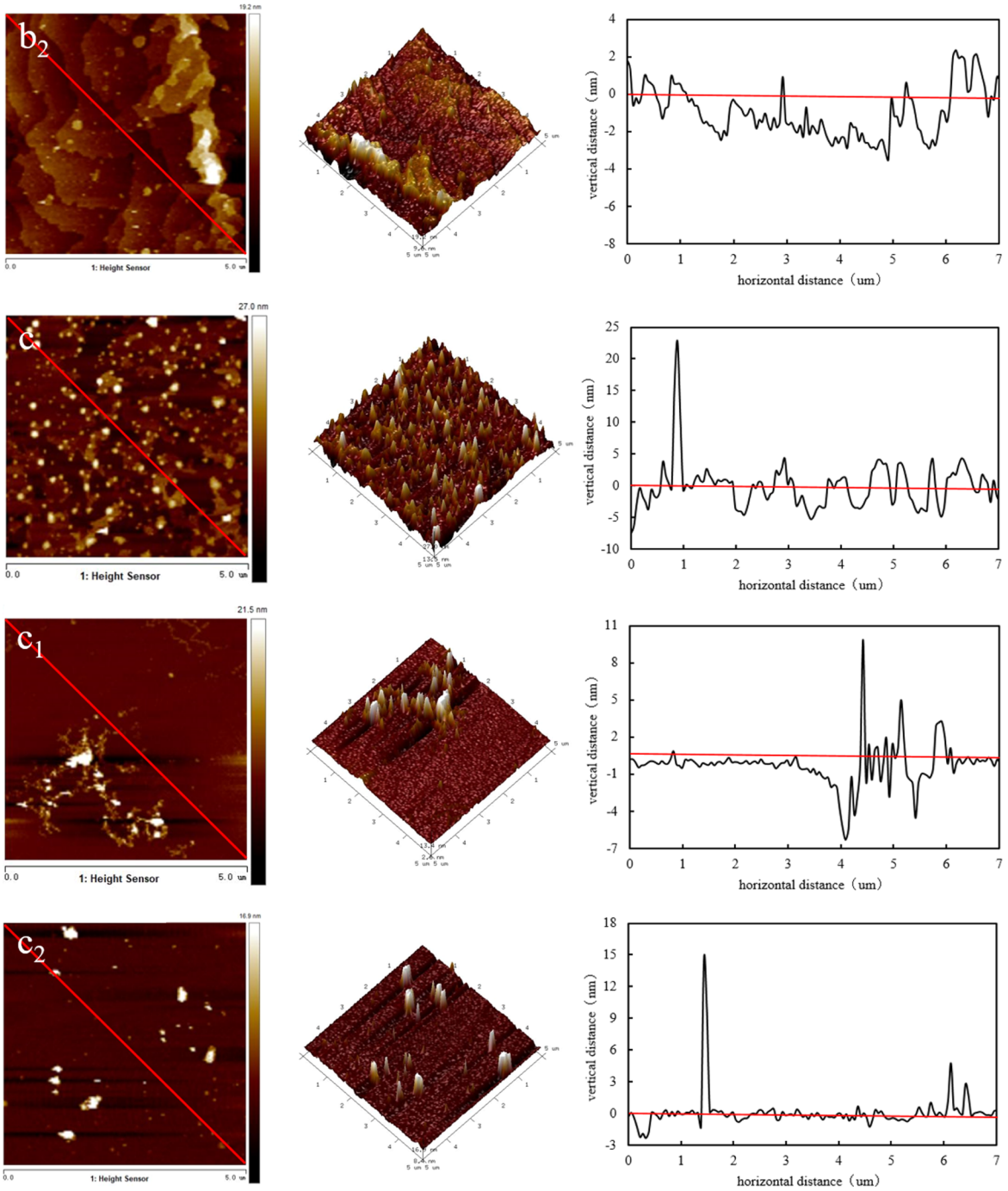

Figure 3. Adsorption topography and height of Gemini surfactants with different carbon chain lengths and Ca^{2+} concentrations: (a) 12-4-12, (a_1) 12-4-12 100 ppm and (a_2) 12-4-12 300 ppm; (b) 14-4-14, (b_1) 14-4-14 100 ppm and (b_2) 14-4-14 300 ppm; and (c) 16-4-16, (c_1) 16-4-16 100 ppm and (c_2) 16-4-16 300 ppm.

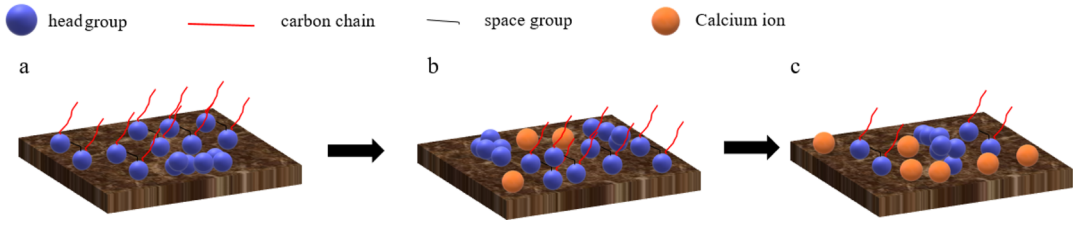

Figure 4. Schematic of surfactant adsorption with the increasing salt concentration: (a) no calcium ions on the surface of the calcite, (b) a small amount of calcium ions contained on the surface of the calcite, and (c) a lot of calcium ions contained on the surface of the calcite.

https://doi.org/10.1021/acsomega.2c01253
ACS Omega 2022, 7, 20768−20778

adhesion means "the work that is required to separate the liquid−solid phases from one another to a certain distance" using the Young−Dupre equation.[35] The adhesion work is the degree of wetting of the rock after wetting. The larger the W_A, the more stable the system. The difference between the two parameters is that the free energy measures the degree to which the solution wets the rock, and the adhesion is the degree of stability of the system after the wetting is completed. The values of both can measure the adsorption ability of the Gemini surfactant.

The varying curve of ΔG at different calcium ion concentration is shown in Figure 5. There is a sharp decrease

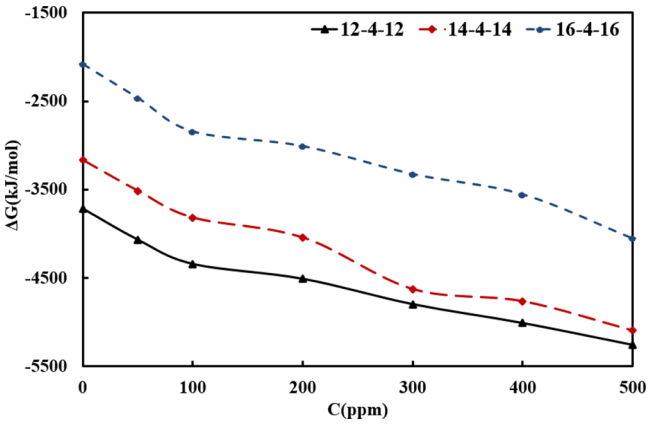

Figure 5. Free energy of the surface vs the calcium ion concentration.

as the Ca^{2+} concentration of the solution is increased. Compared with that of other surfactants, the decline of the free energy of 16-4-16 is the steepest, from −4056.76 to −2084.33 KJ/mol. The curve of the free energy of 14-4-14 decreases from −3169.3 to −5096.53 KJ/mol. The value of change of the free energy of 12-4-12 is the smallest, from −3718.3 to −5257.76 KJ/mol. This means that the added Ca^{2+} promotes the surfactant-containing solution to water-wet.

Moreover, the W_A increases slightly compared with that of the pure solution at the same concentration (as shown in Figure 6). According to the result of the adsorption morphology analysis, it is evident that Ca^{2+} will occupy the rock surface, which decreases the occupying area of the surfactant. Calcium ions are more hydrophilic than surfactants,

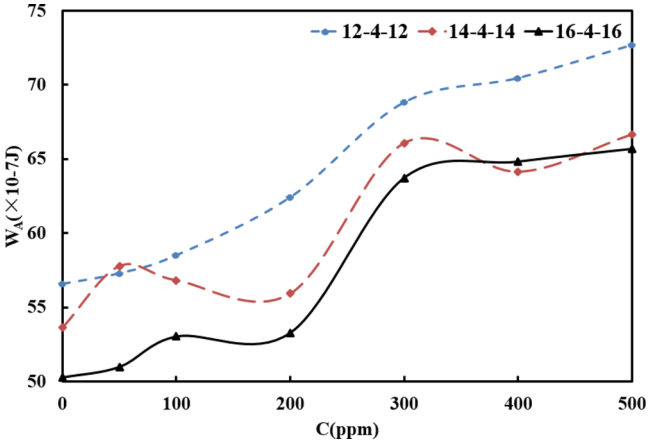

Figure 6. Work of adhesion of cationic Gemini surfactants vs the calcium ion concentration.

so the surface of the rock is more hydrophilic, eventually leading to an increase in the ability of the solution to wet the rock surface. Finally, the ΔG decreases and W_A increases. Although the increase of Ca^{2+} will improve the adsorption ability of the surfactant solution, it is unfavorable for surfactants to prevent hydrogen ions. With the increase of the carbon chain length, the decrease of ΔG gradually increases, which indicates that Ca^{2+} has a significant effect on long-carbon-chain surfactants. However, the short-carbon-chain surfactants are more hydrophilic on the rock surface; the ΔG value is the lowest and the value of W is the highest for 12-4-12. In conclusion, 12-4-12 has the best performance adsorption ability for the rock in a Ca^{2+} environment.

2.5. Static Acid−Rock Reaction. Measurements of the inhibition rate are carried out between the acid solution and calcite to examine the impact of the Gemini surfactant on the reaction rate. There are three components of acid fluids with different Gemini surfactants. The acid system includes 20% HCl, 1% corrosion inhibitor, and 3 times the CMC concentration of the Gemini surfactant. The inhibition rate change is summarized in Table 2. The inhibition rate

Table 2. Inhibition Rates of 12-4-12, 14-4-14, and 16-4-16

type	12-4-12	14-4-14	16-4-16
η (%)	46.34	27.58	13.11

decreased steadily with the increase in the carbon chain length. The inhibition rate of 12-4-12 is 46.34%, which is the highest among the three Gemini surfactants. The inhibition rate of 14-4-14 is 27.58%. The inhibition rate of 16-4-16 is the lowest.

Figure 7 shows the reaction rate of surfactants and the blank group at different times. The reaction rate of surfactants is

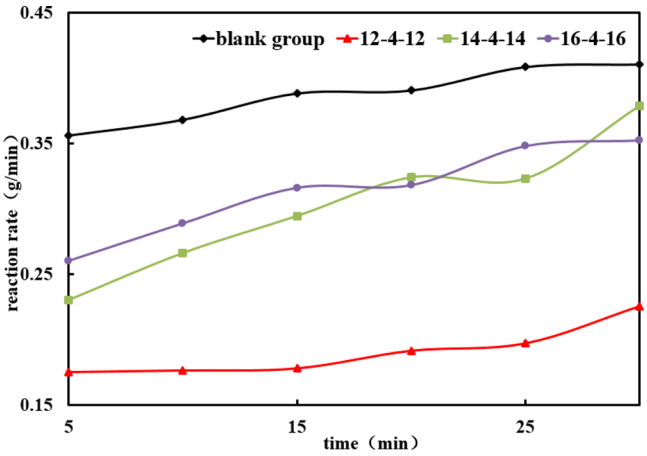

Figure 7. Acid−rock reaction rate at different times.

lower than that of the blank group, which indicates that the surfactant can adsorb on the calcite effectively. Compared with 14-4-14 and 16-4-16, 12-4-12 has the lowest reaction rate at the same time. As the reaction proceeds, the calcium ion concentration increases, and the reaction rate of 12-4-12 remains at a stable value throughout the process. The reaction rates of 14-4-14 and 16-4-16 increase significantly. This result can be explained by the study of adsorption ability and adsorption morphology. Combined with ΔG and W_A, the adsorption ability of 12-4-12 is superior to that of 14-4-14 and

https://doi.org/10.1021/acsomega.2c01253
ACS Omega 2022, 7, 20768−20778

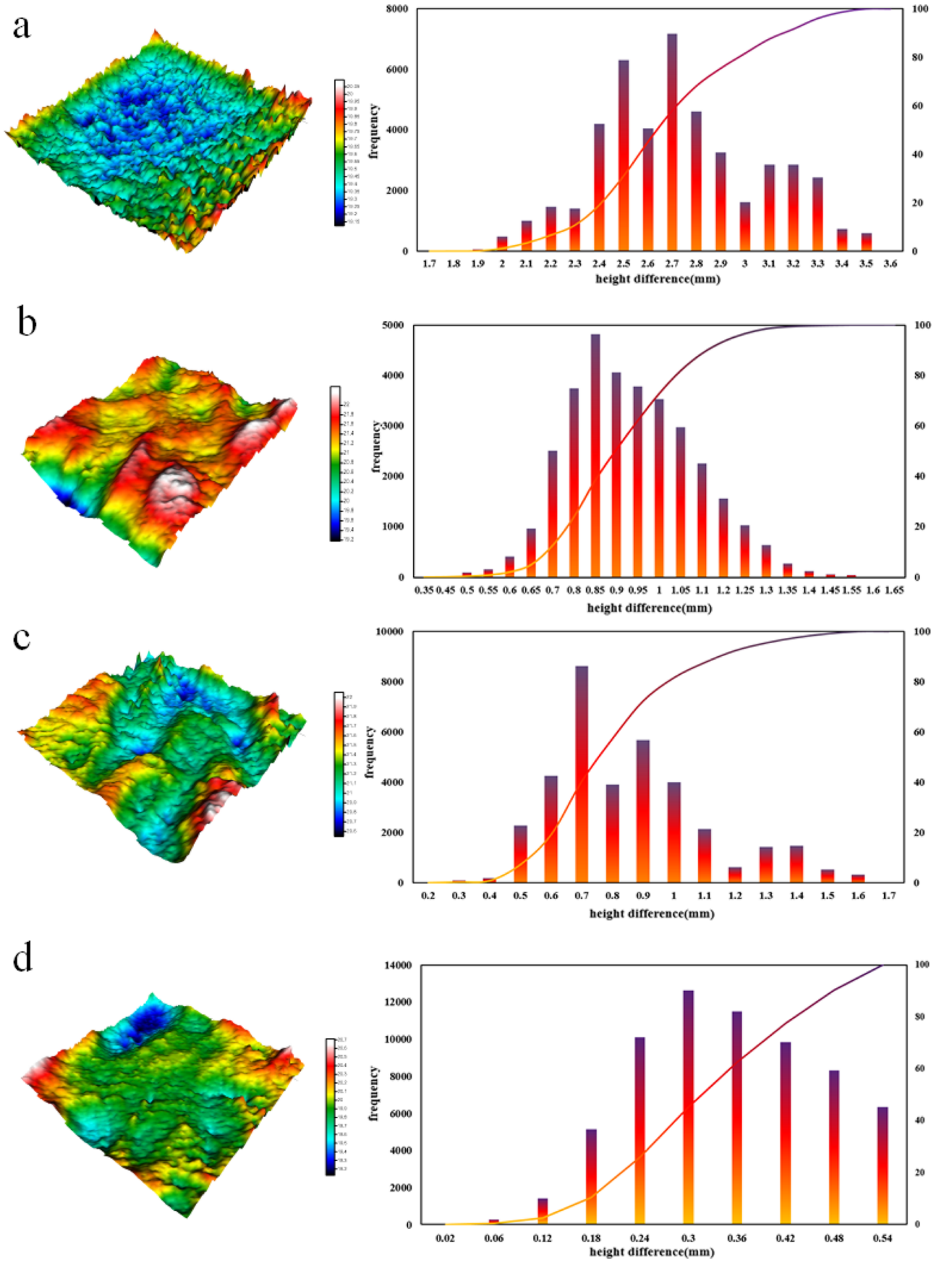

Figure 8. Etched surface morphology and height difference frequency distribution: (a) blank, (b) 12-4-12, (c) 14-4-14, and (d) 16-4-16.

https://doi.org/10.1021/acsomega.2c01253
ACS Omega 2022, 7, 20768−20778

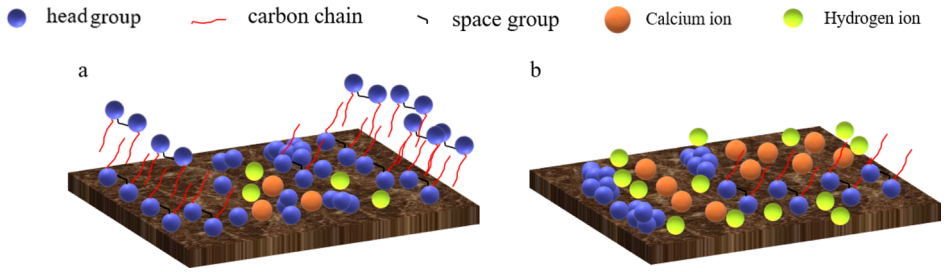

Figure 9. Acid−rock reaction schematic diagram: (a) 12-4-12 and (b) 16-4-16.

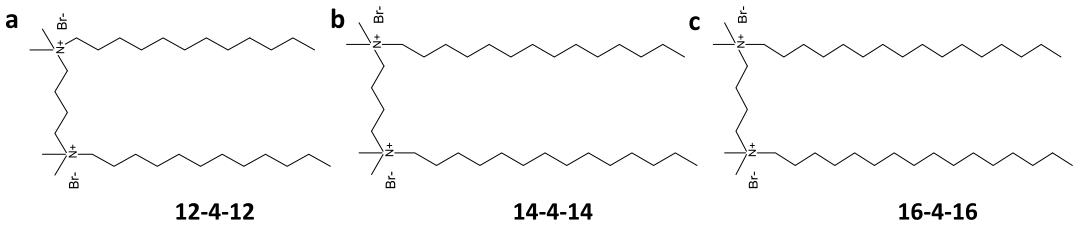

Figure 10. Structure of the Gemini surfactants: (a) 12-4-12, (b) 14-4-14, and (c) 16-4-16.

16-4-16. According to the AFM results, the adsorption area and density for 12-4-12 decrease slightly compared with those of 14-4-14 and 16-4-16 after the addition of the calcium ion concentration. With the increase of calcium ion concentration, the rock surface is occupied by calcium ions, and the aggregation of 14-4-4 and 16-4-16 is gradually strengthened. This leads to a reduced adsorption area; therefore, the ability of the Gemini surfactant to block H^+ is decreased. The surface area of the rock increased gradually as the reaction progressed, which means that the reaction area increased, leading to an increase in the reaction rate. This could also explain why the reaction rate of the blank group increases steadily.

The etched surface morphology is one of the significant factors to influence the carbonate acid fracturing treatment. If the etching pattern is complicated, it is favorable for oil and gas flows.[36,37] To further explore the effect of surfactant adsorption on the surface after etching, the rock surface is digitally characterized after the reaction using laser scanning and three parameters (h_s, $\overline{h}_s$, and S). Figure 8 shows the etched surface morphology and height difference frequency distribution. For the blank group, the average height is 0.341 mm and the standard deviation is 0.124. The shape after etching is relatively uniform, as shown in Figure 8a. However, for 12-4-12, it is apparent that the topography is different from that of the blank group. The surface morphology after etching is extremely nonuniform, and there are many pits and gullies, as shown in Figure 8b. The average height is 2.193 mm; the standard deviation is 0.395. Relatively sharp increases of $\overline{h}_s$ and S are observed after 12-4-12 is adsorbed on the rock surface. Combined with AFM, it can be inferred that surfactant adsorption on the rock surface is uneven. In some areas, the amount of adsorption is large, and the ability to block H^+ is strong, resulting in less erosion and surface bulging in the area. However, as the amount of adsorption is small, H^+ reacts violently with the rock, causing obvious etch pits and grooves on the surface.

For 16-4-16, the average height is 0.81 mm and the standard deviation is 0.234, which are lower than those of 12-4-12(Figure 8b). According to AFM, it can be deduced that surfactant aggregation on the surface becomes obvious with the increase in the concentration of $CaBr_2$ (Figure 9a,b). Thereby, the adsorption area decreases sharply. The ability to block H^+ is weaker than that of 12-4-12. The nonuniformity and higher height difference of the surface make oil and gas flow more favorable after the crack is closed. For 14-4-14, the average height is 0.761 mm. Although the value is slightly smaller than that of 16-4-16, the nonuniformity is higher than that of 16-4-16 according to Figure 8c.

3. CONCLUSIONS

This work set out to provide insights into the effect of Ca^{2+} on the retarding acid−rock reaction rate of the Gemini surfactants with different hydrophobic chains. It is indicated that the CMC decreases with an increase in the Ca^{2+} concentration, showing the expected micelle formation promotion. The salt will reduce the electrostatic repulsion between the intermolecular head groups. As the concentration of Ca^{2+} increases, the morphology is changed significantly for the three Gemini surfactants. An obvious aggregate of the surfactant on the rock is found with the increase in the hydrophobic chain, which results in the decreased density and adsorption area of 14-4-14 and 16-4-16 compared to that of 12-4-12. As $CaBr_2$ is introduced into the solution, the ΔG and W_A results show that 12-4-12 has the best performance in terms of adsorption ability. The static acid−rock reaction reveals that the inhibition rate of 12-4-12 outperforms that of 14-4-14 and 16-4-16. As the reaction progresses, the concentration of calcium ions in the solution increases. Moreover, the reaction rate of the acid solution with the rock gradually increases. The reaction rate of 12-4-12 increases with the slowest rate, indicating that Ca^{2+} has the least impact on its inhibition rate ability, consistent with the AFM and adsorption ability results. Furthermore, the nonuniform surface of the etched rock also proves that there is a densely adsorbed layer of 12-4-12 on the rock. Gemini surfactants can inhibit the acid−rock reaction effectively.

4. EXPERIMENTAL SECTION

4.1. Materials. Chlorhydric acid and $CaBr_2$ are obtained from Chengdu Kelong Chemical. *N*,*N*-Bis(dodecyldimethyl)-1,2-dibromodiammonium diamine (abbreviated as 12-4-12), *N*,*N*-bis(tetradecyldimethyl)-1,2-dibromodiammonium diamine (abbreviated as 14-4-14), and *N*,*N*′-bis-

https://doi.org/10.1021/acsomega.2c01253
ACS Omega 2022, 7, 20768−20778

(hexadecyldimethyl)-1,2-dibromobutylammonium salt (abbreviated as 16-4-16) are synthesized in our laboratory according to the methods given in the previous papers.[29]

The chemical structures of Gemini surfactants are shown in Figure 10. Calcite is used as purchased from Hangzhou Yuhang District Renhe Specimen Factory, and the $CaCO_3$ content is over 99%. All experiments used ultrapure water.

4.2. Surfactant Characterization. A Bruker 400MHZ spectrometer was used to obtain the ^1H NMR spectra and ^{13}C NMR spectra. The specimen is dissolved in a dimethyl sulfoxide solvent in a 5 mm NMR tube. The Gemini surfactant concentration should be moderate to avoid exchange effects and signal-to-noise ratio.[9]

The IR spectroscopy (WOF-530) test was carried out using the KBr tablet method surfactant samples. The IR spectrum test spectral range was 4000−400 cm^{-1}, scan times 16.

4.3. Surface Tension. The surface tension and CMC are determined using the Wilhelmy plate method on a JYW-200A surface tension meter. Before the measurements, the surface tension of distilled water is confirmed to be in the range of 72 + 0.03 mN/m. The measurements are performed until constant surface tension values showed that equilibrium had been reached. Each measurement is performed more than three times, and the standard deviation does not exceed 0.2 mN/m.

4.4. Atomic Force Microscopy. The AFM is performed on a Dimension ICON. For the topography measurements, the rock is soaked in Gemini surfactant aqueous solutions and left for 20 min. Then, the product is taken out and dried under a stable nitrogen flow. All samples are measured three times. The surfactant height on the rock surface is obtained using the Section Analysis module of NanoScope Analysis software.

4.5. Contact Angle Test. The contact angle is measured using the contact angle meter (Dataphysics OCA25). The rock is smoothed using a 600 mesh sandpaper to reduce the roughness of the surface before the experiment. The sessile drop method is used to measure the contact angle. A sessile Gemini surfactant solution droplet of 2 μL is attached carefully to the surface using a pipette. The work of adhesion (W_A) and surface free energy (ΔG) are calculated as follows

$$\Delta G = \frac{RT}{3}\ln\left(\frac{(1-\cos\theta)^2(2+\cos\theta)}{4}\right) \quad (1)$$

where ΔG is the surface free energy, T is the temperature in Kelvin, and R is the universal gas constant (8.314 $Jmol^{-1}$ K^{-1})

$$W_A = \gamma(1+\cos\theta)\times A \quad (2)$$

where γ is the gas−liquid interfacial tension (mN/m), A is the unit area, taken to be 1 cm^2 here, and θ is the contact angle.

4.6. Static Acid−Rock Reaction. The acid system contains 20% HCl and 3 CMC Gemini surfactant. The glue is used to seal the rock to ensure that only one surface can react with the acid system. The rock is taken out every 5 min and dried under nitrogen. The total reaction time is fixed at 30 min. The reaction rate (g/min) and the inhibition rate are calculated using the following equations.

$$v_t = \frac{\Delta m_t}{t} \quad (3)$$

$$v = \frac{m}{t} \quad (4)$$

$$\eta = \frac{v_o - v}{v_o}\times 100\% \quad (5)$$

Δmt(g) is the amount of calcium carbonate dissolved at different times, η is the inhibition rate, ν_o is the reaction rate without the Gemini surfactant, and ν is the reaction rate of the surfactant added.

4.7. Acid-Corroded Rock Surface Test. A 3D laser scanner was used to conduct the digitally shaped topography test after the reaction. Different statistical parameters have been introduced in this paper, which includes the frequency of point data height difference (h_s), average height difference ($\bar{h}_s$), and standard deviation (S).[21]

$$h_s = h - h_{min} \quad (6)$$

$$\bar{h}_s = \sum_{i=1}^{n} h_{si} \quad (7)$$

$$S = \sqrt{\frac{\sum_{i=1}^{n} h_s}{n-1}} \quad (8)$$

h(mm) is the height of each point, h_{min} is the the lowest point of all height points, and $\bar{h}_s$ is the average height difference.

AUTHOR INFORMATION

Corresponding Authors

Shibin Wang − *State Key Laboratory of Oil and Gas Reservoir Geology and Exploitation, Southwest Petroleum University, Chengdu 610500, China;* orcid.org/0000-0002-0152-088X; Email: wangshb07@163.com

Jianchun Guo − *State Key Laboratory of Oil and Gas Reservoir Geology and Exploitation, Southwest Petroleum University, Chengdu 610500, China*; Email: guojianchun@vip.163.com

Authors

Feng Zhao − *State Key Laboratory of Oil and Gas Reservoir Geology and Exploitation, Southwest Petroleum University, Chengdu 610500, China*

Yuheng Yang − *Downhole Operation Company of Xibu Drilling Engineering Company, CNPC, Karamay 834000, China*

Yuan Wang − *Downhole Operation Company of Xibu Drilling Engineering Company, CNPC, Karamay 834000, China*

Zhi Wang − *State Key Laboratory of Oil and Gas Reservoir Geology and Exploitation, Southwest Petroleum University, Chengdu 610500, China*

Peng Shi − *State Key Laboratory of Oil and Gas Reservoir Geology and Exploitation, Southwest Petroleum University, Chengdu 610500, China*

Complete contact information is available at: https://pubs.acs.org/10.1021/acsomega.2c01253

Notes

The authors declare no competing financial interest.

ACKNOWLEDGMENTS

This work was financially supported by the National Science Foundation (U21A20105).

https://doi.org/10.1021/acsomega.2c01253
ACS Omega 2022, 7, 20768−20778

REFERENCES

(1) Menger, F. M.; Littau, C. A. Gemini-Surfactants: Synthesis and Properties. *J. Am. Chem. Soc.* **1991**, *113*, 1451−1452.
(2) Han, Y.; Wang, Y. Aggregation Behavior of Gemini Surfactants and their Interaction with Macromolecules in Aqueous Solution. *Phys. Chem. Chem. Phys.* **2011**, *13*, 1939−1956.
(3) Cao, G.; Guo, X.; Jia, L.; Tian, X. Aggregation Behaviours and Bactericidal Activities of Novel Cationic Surfactants Functionalized with Amides and Ether Groups. *RSC Adv.* **2015**, *5*, 27197−27204.
(4) Zieliński, W.; Wilk, K. A.; Para, G.; Jarek, E.; Ciszewski, K.; Palus, J.; Warszyński, P. Synthesis, Surface Activity and Antielectrostatic Properties of New Soft Dichain Cationic Surfactants. *Colloids Surf., A* **2015**, *480*, 63−70.
(5) Abe, M.; Tsubone, K.; Koike, T.; Tsuchiya, K.; Ohkubo, T.; Sakai, H. Polymerizable Cationic Gemini Surfactant. *Langmuir* **2006**, *22*, 8293−8297.
(6) Rajput, S. M.; Kumar, S.; Aswal, V. K.; El Seoud, O. A.; Malek, N. I.; Kailasa, S. K. Drug-Induced Micelle-to-Vesicle Transition of a Cationic Gemini Surfactant: Potential Applications in Drug Delivery. *Chemphyschem* **2018**, *19*, 865−872.
(7) Taheri-Araghi, S.; Chen, D.; Kohandel, M.; Sivaloganathan, S.; Foldvari, M. Tuning Optimum Transfection of Gemini surfactant-phospholipid-DNA Nanoparticles by Validated Theoretical Modeling. *Nanoscale* **2019**, *11*, 1037−1046.
(8) Zhao, Z.; Guo, X.; Jia, L.; Liu, Y. Synthesis and Properties of Quaternary Ammonium Surfactants Containing a Methoxy Benzyl Substitute. *RSC Adv.* **2014**, *4*, 56918−56925.
(9) Pal, N.; Kumar, N.; Verma, A.; Ojha, K.; Mandal, A. Performance Evaluation of Novel Sunflower Oil-Based Gemini Surfactant(S) with Different Spacer Lengths: Application in Enhanced Oil Recovery. *Energy Fuel.* **2018**, *32*, 11344−11361.
(10) Siddiqui, U. S.; Ghosh, G.; Kabir-ud-Din. Dynamic Light Scattering Studies of Additive Effects on the Microstructure of Aqueous Gemini Micelles. *Langmuir* **2006**, *22*, 9874−9878.
(11) Kabir-Ud-Din; Fatma, W.; Khan, Z. A.; Dar, A. A. H NMR and Viscometric Studies on Cationic Gemini Surfactants in Presence of Aromatic Acids and Salts. *J. Phys. Chem. B* **2007**, *111*, 8860−8867.
(12) Kabir-ud-Din; Fatma, W.; Khatoon, S.; Khan, Z. A.; Naqvi, A. Z. Surface and Solution Properties of Alkanediyl-α,ω-bis-(dimethylcetylammonium bromide) Gemini Surfactants in the Presence of Additives. *J. Chem. Eng. Data* **2008**, *53*, 2291−2300.
(13) Khan, I. A.; Mohammad, R.; Alam, M. S.; Kabir-ud-Din. Effect of Alkylamine Chain Length on the Critical Micelle Concentration of Cationic Gemini Butanediyl-α, ω-bis(dimethylcetylammonium bromide) Surfactant. *J. Dispersion Sci. Technol.* **2009**, *30*, 1486−1493.
(14) Siddiqui, U. S.; Khan, F.; Khan, I. A.; Dar, A. A.; Kabir-ud-Din. Role of added counterions in the micellar growth of bisquaternary ammonium halide surfactant (14-s-14): 1H NMR and viscometric studies. *J. Colloid Interface Sci.* **2011**, *355*, 131−139.
(15) Lamont, R. E.; Ducker, W. A. Surface-Induced Transformations for Surfactant Aggregates. *J. Am. Chem. Soc.* **1998**, *120*, 7602−7607.
(16) Duval, F. P.; Zana, R.; Warr, G. G. Adsorbed Layer Structure of Cationic Gemini and Corresponding Monomeric Surfactants on Mica. *Langmuir* **2006**, *22*, 1143−1149.
(17) Kharisov, R. Y.; Folomeev, A. E.; Sharifullin, A. R.; Bulgakova, G. T.; Telin, A. G. Integrated Approach to Acid Treatment Optimization in Carbonate Reservoirs. *Energy Fuel.* **2011**, *26*, 2621−2630.
(18) Asadollahpour, E.; Baghbanan, A.; Hashemolhosseini, H.; Mohtarami, E. The Etching and Hydraulic Conductivity of Acidized Rough Fractures. *J. Pet. Sci. Eng.* **2018**, *166*, 704−717.
(19) Hou, B.; Zhang, R.; Chen, M.; Kao, J.; Liu, X. Investigation On Acid Fracturing Treatment in Limestone Formation Based On True Tri-Axial Experiment. *Fuel* **2019**, *235*, 473−484.
(20) Jafarpour, H.; Moghadasi, J.; Khormali, A.; Petrakov, D. G.; Ashena, R. Increasing the Stimulation Efficiency of Heterogeneous Carbonate Reservoirs by Developing a Multi-Bached Acid System. *J. Pet. Sci. Eng.* **2019**, *172*, 50−59.
(21) Li, Q.; Chen, W.; Lu, Y.; Xiao, Q. Etched Surface Morphology Analysis Experiments Under Different Reaction Rates. *J. Pet. Sci. Eng.* **2019**, *172*, 517−526.
(22) Wang, S.; Zhang, D.; Guo, J.; Guan, B. Experiment and Analysis of the Reaction Kinetics of Temperature Control Viscosity Acids with Limestone. *J. Pet. Sci. Eng.* **2018**, *165*, 305−312.
(23) Siddiqui, S.; Nasr-El-Din, H. A.; Khamees, A. A. Wormhole Initiation and Propagation of Emulsified Acid in Carbonate Cores Using Computerized Tomography. *J. Pet. Sci. Eng.* **2006**, *54*, 93−111.
(24) Gomaa, A. M.; Nasr-El-Din, H. A. Effect of Elastic Properties On the Propagation of Gelled and In-Situ Gelled Acids in Carbonate Cores. *J. Pet. Sci. Eng.* **2015**, *127*, 101−108.
(25) Yuan, L.; Wang, Y.; Li, Q.; Chen, K.; Li, Y. Evaluation of a Control-Released In-Situ Generated Acid Tablet for Acid Fracturing. *J. Pet. Sci. Eng.* **2019**, *174*, 384−393.
(26) Adewunmi, A. A.; Solling, T.; Sultan, A. S.; Saikia, T. Emulsified acid systems for oil well stimulation: A review. *J. Pet. Sci. Eng.* **2022**, *208*, 109569.
(27) Liu, M.; Zhang, S.; Mou, J.; Zhou, F.; Shi, Y. Diverting Mechanism of Viscoelastic Surfactant-Based Self-Diverting Acid and its Simulation. *J. Pet. Sci. Eng.* **2013**, *105*, 91−99.
(28) Yousufi, M. M.; Elhaj, M. E. M.; Moniruzzaman, M.; Ayoub, M. A.; Nazri, A. B. M.; Husin, H. B.; Saaid, I. B. M. Synthesis and Evaluation of Jatropha Oil-Based Emulsified Acids for Matrix Acidizing of Carbonate Rocks. *J. Pet. Explor. Prod. Technol.* **2019**, *9*, 1119−1133.
(29) Zhao, F.; Wang, S.; Shen, X.; Guo, J.; Liu, Y. Study On Mechanism of Gemini Surfactant Inhibiting Acid Rock Reaction Rate. *Colloids Surf., A* **2019**, *578*, 123629.
(30) Shen, X.; Wang, S.; Guo, J.; Chen, F.; Xu, B.; Wang, Z.; Liu, Y. Effect of Carbon Chain Lengths of Cationic Surfactant On Inhibition Rate of Acid-Rock Reaction. *J. Pet. Sci. Eng.* **2021**, *196*, 107793.
(31) Song, L. D.; Rosen, M. J. Surface Properties, Micellization, and Premicellar Aggregation of Gemini Surfactants with Rigid and Flexible Spacers. *Langmuir* **1996**, *12*, 1149−1153.
(32) Wang, X.; Li, Y.; Li, J.; Wang, J.; Wang, Y.; Guo, Z.; Yan, H. Salt Effect On the Complex Formation Between Polyelectrolyte and Oppositely Charged Surfactant in Aqueous Solution. *J. Phys. Chem. B* **2005**, *109*, 10807−10812.
(33) Rehman, J.; Ponce, C. P.; Araghi, H. Y.; Paige, M. F. Cation Binding Properties of an Anionic Gemini Surfactant Monolayer. *Colloids Surf., A* **2017**, *522*, 536−543.
(34) Extrand, C. W. A Thermodynamic Model for Wetting Free Energies From Contact Angles. *Langmuir* **2003**, *19*, 646−649.
(35) Koopal, L. K. Wetting of Solid Surfaces: Fundamentals and Charge Effects. *Adv. Colloid Interface Sci.* **2012**, *179−182*, 29−42.
(36) Liu, F.; Ma, H.; Li, L.; Zhou, C.; Luo, Z.; Gao, X.; Wu, Y. Acid-Etched Fracture Length and Conductivity Experiments with Relayed Large-Scale Rock Plates. *J. Pet. Sci. Eng.* **2021**, *196*, 107978.
(37) Zhang, L.; Zhou, F.; Mou, J.; Xu, G.; Zhang, S.; Li, Z. A New Method to Improve Long-Term Fracture Conductivity in Acid Fracturing Under High Closure Stress. *J. Pet. Sci. Eng.* **2018**, *171*, 760−770.

https://doi.org/10.1021/acsomega.2c01253
ACS Omega 2022, 7, 20768−20778